

COMPLEX SINGULARITIES OF THE AMPLITUDES OF DIRECT NUCLEAR REACTIONS

L. D. BLOKHINTSEV, É. I. DOLINSKIĬ, and V. S. POPOV

Institute of Nuclear Physics, Moscow State University and Institute of Theoretical and Experimental Physics

Submitted to JETP editor July 24, 1962

J. Exptl. Theoret. Phys. (U.S.S.R.) **43**, 2290-2298 (December, 1962)

Rules for determining the complex singularities on the physical sheet of the amplitudes of nonrelativistic single-loop graphs are indicated. A classification of the complex singularities of nonrelativistic triangular graphs with arbitrary masses is given. It is shown with triangular graphs for direct nuclear reactions of the type $A + x \rightarrow B + y + z$ as an example that the complex singularities in the momentum transfer t_{xy} may lie close to the physical region. A single analytic expression for the amplitude F_{31} of a triangular graph is derived and the asymptotic behavior of F_{31} for values of t_{xy} far away from the singular point is investigated.

1. INTRODUCTION

THE dispersion theory of direct nuclear reactions is based on the assumption that the direct processes are due to the presence of singularities of the reaction amplitude in the momentum transfer. The contribution of each singular point to the amplitude is described by a Feynman graph.^[1,2] It has been observed earlier^[3] that the analytic properties of the amplitudes of direct processes at low and intermediate energies are determined by the singularities of the graphs with $n \geq 5l/2$ alone.¹⁾ These singularities are found with the help of the nonrelativistic Landau equations considered by us earlier^[4,5] and are, for $n > 5l/2$, identical with the singularities of the corresponding nonrelativistic graphs.²⁾ Equations for the singular surfaces of nonrelativistic single-loop graphs have been given in^[4,5]; there also conditions for the existence of real singularities on the physical sheet of the amplitude are given. However, the reaction amplitudes may have complex singularities as well as real ones on the physical sheet, as was demonstrated in^[6] for the reaction $N + \pi \rightarrow N + 2\pi$.

In the present paper we discuss the problem of the complex singularities of nonrelativistic single-loop graphs. It is shown, using as an example the nuclear reaction of the type $A + x \rightarrow B + y + z$, that the complex singularities in the momentum

transfer of the amplitude corresponding to a triangular graph may lie close to the physical region. The investigation of the complex singularities may therefore be important for the now-developing dispersion theory of direct nuclear reactions.

2. COMPLEX SINGULARITIES OF NONRELATIVISTIC SINGLE-LOOP GRAPHS

We shall start from the integral representation for the amplitude $F_{n1}(\eta_{ij})$ of a nonrelativistic single-loop graph with constant vertices, obtained in^[4,5]:

$$F_{n1}(\eta_{ij}) = C_{n1} \int_0^1 \prod_{i=1}^n dx_i \delta\left(\sum_{k=1}^n \alpha_k - 1\right) \times \delta\left(\sum_{i=1}^n \omega_i m_i x_i\right) (X - i\delta)^{-(n-5/2)}, \quad \delta \rightarrow +0; \quad (1)$$

$$X = \sum_{i,j=1}^n \alpha_i \alpha_j \omega_i \omega_j m_i m_j \eta_{ij}. \quad (2)$$

Here η_{ij} are the external kinematic invariants introduced in^[4,5] and $\omega_i = \pm 1$ indicates the direction of the i -th internal line of the graph. The condition $\delta \rightarrow +0$, coming from Feynman's rule for circumventing the poles of the nonrelativistic Green's function, defines the contour of integration over the α_i , around the singular points of the integrand in (1), and thus defines the physical branch of the amplitude F_{n1} .

The rules for singling out the real singularities of $F_{n1}(\eta_{ij})$ on the physical sheet have been given in^[4,5]. However, since these rules presuppose

¹⁾ n is the number of internal lines of the graph, and l the number of independent closed loops.

²⁾ Nonrelativistic graphs are Feynman graphs with nonrelativistic propagators.

that the α_i are positive at a real singular point of F_{n1} on the physical sheet (cf. [7,8]), they cannot be used to find the complex physical singularities of F_{n1} .

Employing the method of Landshoff and Treiman, [6] we consider below a different method for determining the physical singularities of F_{n1} , which is also applicable to complex singularities. For graphs with $n \leq 5$, in which case all η_{ij} are independent, we may use the fact that the α_i in (1) and (2) are positive at a real physical singularity of $F_{n1}(\eta_{ij})$ and associate the infinitesimal imaginary parts with the quantities η_{ij} themselves:

$$\eta_{ij} \rightarrow \eta_{ij} - i\omega_i\omega_j \delta_{ij}, \tag{3}$$

where $\delta_{ij} \rightarrow +0$ all independently. (For $n \geq 6$ there is a relation between the η_{ij} , but, as shown by Brown, [9] single-loop graphs with $n \geq 6$ have no proper singularities, but only singularities associated with the "contracted" graphs with $n \leq 5$). The equation for the singular surface of a single-loop graph is a quadratic equation in each of the variables η_{ij} . [4,5] Solving it for some particular η_{ij} , we find two roots:

$$\eta_{ij}^{(\pm)} = K_{ij}^{(\pm)}(\eta_{i'j'}), \quad (i', j') \neq (i, j). \tag{4}$$

Let us consider the analytic continuation of the amplitude $F_{n1}(\eta_{ij})$ along the real axis of the variable η_{ij} for fixed values of the remaining variables $\eta_{i'j'}$. If we encounter a singularity ($\eta_{ij}^{(+)}$ or $\eta_{ij}^{(-)}$) on the path of the analytic continuation, rule (3) tells us how to deform the contour in order to remain on the physical sheet of F_{n1} . Since the deformation of the path of the analytic continuation is equivalent to a displacement of the singularity into the complex plane of the variable η_{ij} in the opposite direction, we obtain the following rule:

At a real singularity of the amplitude $F_{n1}(\eta_{ij})$ on the physical sheet the sign of $\text{Im } K_{ij}^{(\pm)}(\eta_{i'j'} - i\omega_{i'}\omega_{j'}\delta_{i'j'})$ must coincide with the sign of $\omega_i\omega_j$; this condition must be satisfied for all i, j . (5)

Let us illustrate the rule (5) by the example of a triangular graph. We consider the graph of Fig. 1b and find its real singularities in the variable η_{23} . According to [4] we have

$$\eta_{23}^{\pm} = K_{23}^{(\pm)} = \eta_{12} + \eta_{13} \pm 2\sqrt{\eta_{12}\eta_{13}}.$$

Rule (5) gives the sign

$$\text{Im } K_{23}^{(\pm)}(\eta_{12} + i\delta, \eta_{13} - i\delta') = \omega_2\omega_3 = -1$$

where $\delta, \delta' \rightarrow +0$. This leads to the inequalities

$$1 \pm \eta_{13}/\sqrt{\eta_{12}\eta_{13}} < 0, \quad 1 \pm \eta_{12}/\sqrt{\eta_{12}\eta_{13}} > 0,$$

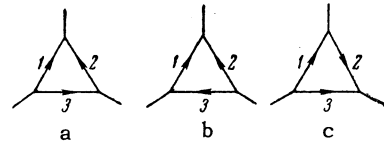


FIG. 1

which imply that the real singularity on the physical sheet is η_{23}^- for $\eta_{13} > \eta_{12} > 0$ and η_{23}^+ for $\eta_{13} < \eta_{12} < 0$. This agrees with the results of [4,5]. The rule (5) simplifies considerably the selection of the real physical singularities.

The complex singularities of $F_{n1}(\eta_{ij})$ can be discussed in the general case with the help of the method of Tarski. [10] We shall, however, restrict ourselves to the most important case for our purposes, viz., where only one of the variables η_{ij} is complex at the singular point. Let us first consider such values of $\eta_{i'j'}$ for which there exists a real singularity in η_{ij} on the physical sheet, given by (4) and (5). Changing the variables $\eta_{i'j'}$, we go from a real to a complex singularity in η_{ij} in such a way that the singular point, displaced from the real axis into the η_{ij} plane according to (4) and (5), is continuously transferred to the surface of complex singularities without intersecting the real axis of η_{ij} . This leads to the following rule for selecting the complex physical singularities:

For the branch of the complex singular surface lying on the physical sheet, $\text{sign } \text{Im } K_{ij}^{(\pm)}(\eta_{i'j'}) = \omega_i\omega_j$ in the neighborhood of every limiting point separating the real and complex singularities of the amplitude. (6)

Let us consider the complex singularities of the amplitude F_{31} of a triangular graph, using the rule (6). Let η_{12} have a fixed real value. Then (4) defines, in the real (η_{13}, η_{23}) plane, a parabola with the axis along the line $\eta_{13} = \eta_{23}$ which intersects the coordinate axes in the points $(\eta_{12}, 0)$ and $(0, \eta_{12})$. Only those parts of this parabola which are indicated in Table I of the earlier paper [4] correspond to physical singularities. The curve for the real physical singularities in the (η_{13}, η_{23}) plane terminates at the points of intersection $(0, \eta_{12})$ or $(\eta_{12}, 0)$, corresponding to the normal threshold in the variables η_{13} or η_{23} .

In going through the normal threshold, the singularity becomes complex. The physical branch for it is easily selected with the help of the rule (6). For example, for the graph of Fig. 1a with

³On other branches of the complex singular surface, the condition (6) may be violated.

$\eta_{12} < 0$, the real physical curve is, according to [4],

$$\eta_{23} = \eta_{23}^- = -(|\eta_{12}|^{1/2} + |\eta_{13}|^{1/2})^2$$

(with $\eta_{13} < 0$). This curve terminates in the point $\eta_{13} = 0, \eta_{23} = \eta_{12} < 0$ (see Fig. 2a). For $\eta_{13} > 0, \eta_{12} < 0$, only the branch $\eta_{23} = \xi_{23}^+$ of the two branches of the complex singularity curve $\eta_{23} = \xi_{23}^\pm$, where

$$\xi_{23}^\pm = \eta_{12} + \eta_{13} \pm 2i(-\eta_{12}\eta_{13})^{1/2} \text{ with } \eta_{12}\eta_{13} < 0, \quad (7)$$

satisfies condition (6), $\text{Im } \xi_{23}^+ > 0$, and is, therefore, the complex singular curve on the physical sheet.

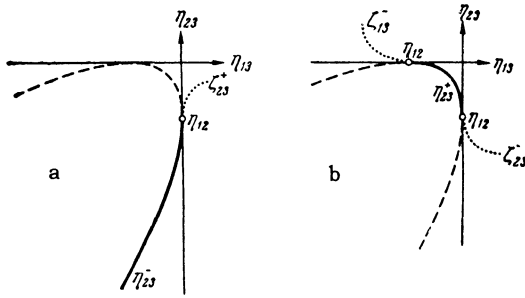


FIG. 2. Curves of the real and complex singularities of the amplitude F_{31} of a triangular graph: a—graph of Fig. 1a with $\eta_{12} < 0$, b—graph of Fig. 1c with $\eta_{12} < \eta_{13} < 0$. The solid curve is the curve of the real singularities of F_{31} on the physical sheet, the dashed curve is the curve of the real singularities not lying on the physical sheet, and the dotted curve represents schematically the positions of the complex singularities on the physical sheet.

In the case of the graph of Fig. 1c, the real physical singular curve for $\eta_{12} < \eta_{13} < 0$ is $\eta_{23} = \eta_{23}^+ = -(|\eta_{12}|^{1/2} - |\eta_{13}|^{1/2})^2$ (see Fig. 2b). At the limiting point $\eta_{13} = 0, \eta_{23} = \eta_{12}$ the amplitude develops a complex singularity in the variable η_{13} , and at the point $\eta_{23} = 0, \eta_{13} = \eta_{12}$, a complex singularity in the variable η_{23} . The physical branches are, according to (6), determined by the conditions $\text{Im } \xi_{23}^\pm < 0$ and $\text{Im } \xi_{13}^\pm < 0$. This leads to the follow-

ing curves for the complex singularities on the physical sheet:

$$\begin{aligned} \eta_{23} &= \xi_{23}^- = \eta_{12} + \eta_{13} \\ &\quad - 2i(-\eta_{12}\eta_{13})^{1/2} \text{ for } \eta_{12} < 0, \eta_{13} > 0, \\ \eta_{13} &= \xi_{13}^- = \eta_{12} + \eta_{23} \\ &\quad - 2i(-\eta_{12}\eta_{23})^{1/2} \text{ for } \eta_{12} < 0, \eta_{23} > 0. \end{aligned}$$

The other cases are treated in an analogous fashion.

The results for the graph of Fig. 1a are given in the table. Together with Table I of [4], it gives a complete classification of the physical singularities of the amplitude F_{31} for a triangular graph in which two of the three variables η_{ij} are real.

Let us consider some examples of complex singularities of triangular graphs in the theory of direct nuclear reactions. A three-ray vertex (i, j) with nuclear-stable particles satisfies the condition $\eta_{ij} < 0$. [4,5] Therefore, a triangular graph for the simplest reaction of the type $A + x \rightarrow B + y$ has only real singularities. Complex singularities occur in the more complicated reactions of the type $A + x \rightarrow B + y + z$. The corresponding graph is shown in Fig. 3.

The relation between the variables η_{ij} and the nonrelativistic kinematic invariants s_{ij}, t_{ij} for the graph of Fig. 3 follows from Eqs. (34) and (35) of [5]:

$$\begin{aligned} \eta_{12} &= \frac{1}{2m_1m_2} [s_{Bz} - 2(M_B + M_z) Q_{12}], \quad \eta_{13} = -\frac{M_A}{m_1m_3} Q_{13}, \\ \eta_{23} &= -\frac{1}{2m_2m_3} [t_{xy} + 2(M_x - M_y) Q_{23}]; \\ Q_{12} &= m_1 + m_2 - M_B - M_z, \quad Q_{13} = m_1 + m_3 - M_A, \\ Q_{23} &= M_x + m_3 - M_y - m_2. \end{aligned} \quad (8)$$

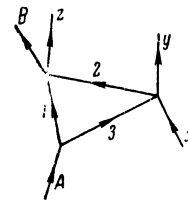


FIG. 3

Complex singularities on the physical sheet of the amplitude F_{31} of a nonrelativistic triangular graph (see Fig. 1a)

Variable η_{ij} , in terms of which there exists a complex singularity on the physical sheet	Condition for the existence of a complex singularity	Position of the complex singularity
η_{23} (first class vertex)	$\eta_{12}\eta_{13} < 0$	$\eta_{23} = \xi_{23}^+ = \eta_{12} + \eta_{13} + 2i(-\eta_{12}\eta_{13})^{1/2}$
η_{13} (second class vertex)	$\eta_{12}\eta_{23} < 0$	$\eta_{13} = \xi_{13}^- = \eta_{12} + \eta_{23} - 2i(-\eta_{12}\eta_{23})^{1/2}$
η_{12} (second class vertex)	$\eta_{13}\eta_{23} < 0$	$\eta_{12} = \xi_{12}^- = \eta_{13} + \eta_{23} - 2i(-\eta_{13}\eta_{23})^{1/2}$

The formulas defining the kinematics of a five-tailed graph are obtained in much the same way as the formulas (39) of [5] for a four-tailed graph, and are of the form

$$t_{xy} = -(\sqrt{M_y/M_x} \mathbf{p} - \sqrt{M_x/M_y} \mathbf{p}')^2;$$

$$p = \frac{1}{2} [(1 - \xi^2) s_{Ax}]^{1/2},$$

$$p' = \frac{1}{2} [(1 - \xi'^2) (s_{Ax} + 2(M_A + M_x)(Q - T_{Bz}))]^{1/2};$$

$$\xi = (M_A - M_x) / (M_A + M_x),$$

$$\xi' = (M_B + M_z - M_y) / (M_B + M_z + M_y); \quad (9)$$

where

$$Q = M_A + M_x - (M_B + M_y + M_z)$$

is the energy of the reaction, and

$$s_{Ax} = 2(M_A + M_x) T_{Ax} = 2M_A E_x, \quad s_{Bz} = 2(M_B + M_z) T_{Bz}.$$

Here $T_{Ax}(T_{Bz})$ is the kinetic energy of the relative motion of particles A, x(B, z) in their center of mass system, and E_x is the kinetic energy of the incident particle x in the laboratory system (in which A is at rest).

Since $\eta_{13} < 0$, complex singularities in t_{xy} will occur for $\eta_{12} > 0$. We find from (8) that for $Q_{12} > 0$ and values of T_{Bz} such that $0 \leq T_{Bz} < Q_{12}$, the graph of Fig. 3 has a real singularity in t_{xy} , which becomes complex when $T_{Bz} > Q_{12}$. If $Q_{12} < 0$, there will be a complex singularity in t_{xy} for any value of T_{Bz} . For a given energy of the incident particles A, x, the value of T_{Bz} may vary within the limits

$$0 \leq T_{Bz} \leq \bar{T}_{Bz} = s_{Ax} / 2(M_A + M_x) + Q. \quad (10)$$

The position of the singularity in t_{xy} depends, besides the masses of the particles, also on the value of the kinetic energy T_{Bz} .

Figures 4 and 5 show the position of the physical

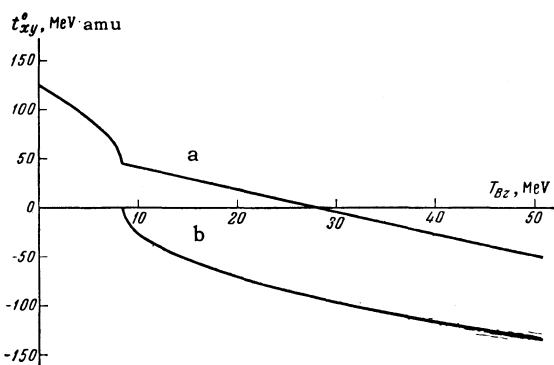


FIG. 4. Position of the physical singularity in t_{xy} for the reaction $N^{14} + d \rightarrow N^{14} + n + p$ (triangular graph of Fig. 3, with $A = B \rightarrow N^{14}$, $x \rightarrow d$, $y \rightarrow n$, $z \rightarrow p$, $1 \rightarrow N^{13}$, $2 \rightarrow d$, $3 \rightarrow n$). Curve a: $\text{Re } t_{xy}^0$, curve b: $\text{Im } t_{xy}^0$.

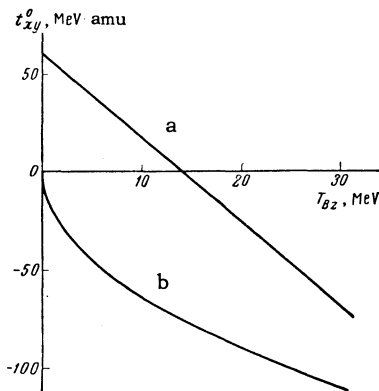
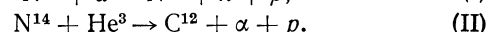
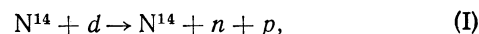


FIG. 5. Position of the physical singularities in t_{xy} for the reaction $N^{14} + \text{He}^3 \rightarrow \text{C}^{12} + \alpha + p$ (graph of Fig. 3, with $A \rightarrow N^{14}$, $B \rightarrow \text{C}^{12}$, $x \rightarrow \text{He}^3$, $y \rightarrow \alpha$, $z \rightarrow p$, $1 \rightarrow \text{C}^{12}$, $2 \rightarrow p$, $3 \rightarrow d$). Curve a: $\text{Re } t_{xy}^0$, curve b: $\text{Im } t_{xy}^0$.

singularity in t_{xy} of the simplest triangular graphs for the reactions



The poles in t_{xy} for these reactions lie at the following points: $t_{xy}^0 = 4.46$ MeV amu [reaction (I), pole graph with a proton in the intermediate state] and $t_{xy}^0 = 41.5$ MeV amu [reaction (II), pole graph with a neutron in the intermediate state].

The dependence of \bar{T}_{Bz} on the kinetic energy of particle x in the l.s. is given by the formulas

$$\bar{T}_{Bz} = 0.875 E_x - 2.23, \quad (\text{I}')$$

$$\bar{T}_{Bz} = 0.824 E_x + 8.06 \quad (\text{II}')$$

(\bar{T}_{Bz} and E_x in MeV).

The physical region for t_{xy} is given by $t_{xy} < 0$, with the upper limit $\bar{t}_{xy} = 0$ independently of the value of T_{Bz} for reaction (I). For reaction (II), \bar{t}_{xy} moves into the region of negative values as T_{Bz} increases, but $\bar{t}_{xy} > -5$ MeV amu as long as $T_{Bz} \leq 50$ MeV. It follows from Figs. 4 and 5 that the complex singularities in the square of the momentum transfer t_{xy} , of the simplest triangular graphs for direct reactions of the type $A + x \rightarrow B + y + z$ may lie closer to the physical region than the real singularities of more complicated graphs (see Table II of [5]). In reactions with $Q_{12} > 0$ [cf. formula (8)], there may be real as well as complex singularities in t_{xy} at one and the same energy of the initial particles, depending on the kinetic energy of the relative motion of the particles B and z. Analogous results are found for triangular graphs for more complicated reactions than $A + x \rightarrow B + y + z$.

3. ANALYTIC PROPERTIES AND ASYMPTOTIC FORM OF THE AMPLITUDE FOR A TRIANGULAR GRAPH

An explicit expression for the amplitude $F_{31}(\eta_{ij})$ of a triangular graph with constant vertices was ob-

tained in [4,5]. The function $F_{31}(\eta_{ij})$ was given by different formulas in the different regions of the variables η_{ij} . Using the results of Sec. 2, we may find a single analytic expression for $F_{31}(\eta_{ij})$:

$$F_{31}(\eta_{ij}) = C_{31}(\eta_{23}^0 - \xi_{23})^{-1/2} \varphi(z); \quad (11)$$

$$C_{31} = i\pi^3 \left[\frac{2}{m_2 m_3 (m_1 + m_2) (m_1 + m_3)} \right]^{1/2}, \quad \varphi(z) = \frac{1}{2\sqrt{z}} \ln \frac{1 + \sqrt{z}}{1 - \sqrt{z}}, \quad (12)$$

$$z = \frac{\eta_{23} - \eta_{23}^0}{\xi_{23} - \eta_{23}^0},$$

$$\eta_{23}^0 = m_1(m_2 - m_3) \left[\frac{\eta_{13}}{m_2(m_1 + m_3)} - \frac{\eta_{12}}{m_3(m_1 + m_2)} \right], \quad (13)$$

where ξ_{23} denotes the position of the physical singularity (real or complex):

$$\xi_{23} = \begin{cases} \eta_{23}^- = \eta_{12} + \eta_{13} - 2(\eta_{12}\eta_{13})^{1/2} & \eta_{12} < 0, \eta_{13} < 0 \\ \xi_{23}^+ = \eta_{12} + \eta_{13} + 2i(-\eta_{12}\eta_{13})^{1/2} & \eta_{12}\eta_{13} < 0 \\ \eta_{23}^+ = \eta_{12} + \eta_{13} + 2(\eta_{12}\eta_{13})^{1/2} & \eta_{12} > 0, \eta_{13} > 0 \end{cases} \quad (14)$$

In formula (11) we have

$$(\eta_{23}^0 - \xi_{23})^{1/2} = (\omega_{23} | \eta_{12} |)^{1/2} + (\omega_{23}^{-1} | \eta_{13} |)^{1/2} \text{ при } \eta_{12} < 0, \eta_{13} < 0,$$

where

$$\omega_{23} = m_2(m_1 + m_3) / m_3(m_1 + m_2). \quad (15)$$

The value of $(\eta_{23}^0 - \xi_{23})^{1/2}$ in the other regions of η_{12}, η_{13} is obtained by analytic continuation around the normal threshold in η_{12} or η_{13} according to (3). As a result we find

$$(\eta_{23}^0 - \xi_{23})^{1/2} = \begin{cases} (\omega_{23} | \eta_{12} |)^{1/2} + (\omega_{23}^{-1} | \eta_{13} |)^{1/2} & \eta_{12} < 0, \eta_{13} < 0 \\ (\omega_{23} | \eta_{12} |)^{1/2} - i(\omega_{23}^{-1} | \eta_{13} |)^{1/2} & \eta_{12} < 0, \eta_{13} > 0 \\ -i(\omega_{23} \eta_{12})^{1/2} + (\omega_{23}^{-1} | \eta_{13} |)^{1/2} & \eta_{12} > 0, \eta_{13} < 0 \\ -i[(\omega_{23} \eta_{12})^{1/2} + (\omega_{23}^{-1} | \eta_{13} |)^{1/2}] & \eta_{12} > 0, \eta_{13} > 0 \end{cases} \quad (16)$$

The function $\varphi(z)$ is analytic in the complex z plane with the cut $1 \leq z < \infty$. The branches of the functions \sqrt{z} and $\ln z$ in (12) are chosen in such a way that $\varphi(z)$ takes on real values for $-\infty < z < 1$. We note that $\varphi(0) = 1$ and $\varphi(z) \sim \frac{1}{2} \ln(1/1-z)$ for $z \rightarrow 1$. If $|z| \gg 1$, we have $\varphi(z) \sim \pi/2\sqrt{z}$.

We emphasize that formulas (11) to (14) refer to the graph of Fig. 1a, in which the vertex (2, 3) is of the first class, i.e., $\omega_2\omega_3 = 1$. [4,5] It is seen from Fig. 1 that, in nonrelativistic triangular graphs, there is always one vertex of the first class and two of the second class. The physical difference between the vertices of different classes lies in the circumstance that a triangular graph cannot be contracted along a line opposite a first class vertex, since this would lead to a graph in

which all internal lines are directed in the same sense. Such a graph vanishes in the nonrelativistic theory. [4,5] Therefore, the normal threshold $\eta_{ij} = 0$ in a variable η_{ij} corresponding to a vertex (i, j) of the first class is not a singular point of the amplitude $F_{31}(\eta)$.

Owing to this fact, the analytic properties of the amplitude $F_{31}(\eta)$ are much simpler than in the relativistic case. We are able to give an explicit expression for $F_{31}(\eta)$ in contradistinction to the relativistic case, where one can determine only the imaginary part of the amplitude $F_{31}(\eta)$ of a triangular graph with arbitrary masses [11] or the sum of the derivatives of the amplitude with respect to the squares of the internal masses. [12,13] The variables η_{ij} corresponding to vertices of the first and the second class enter in the expression for $F_{31}(\eta_{ij})$ in different ways. Thus, in Fig. 2a, the singularities of the amplitude $F_{31}(\eta_{ij})$ lie on the curve $\eta_{23} = \eta_{23}^-$ and on the straight line $\eta_{13} = 0$. Therefore, if the amplitude $F_{31}(\eta_{ij})$ of the graph of Fig. 1a as an analytic function of η_{23} has only the anomalous threshold singularity $\eta_{23} = \eta_{23}^-$, it has, as a function of η_{13} for fixed η_{12}, η_{23} , two singular points. Expressions for $F_{31}(\eta_{ij})$ corresponding to the graphs of Figs. 1b and c are obtained from (11) to (14) by an appropriate change of indices, with η_{23} replaced by that variable η_{ij} which corresponds to the first class vertex.

Let now one of the variables η_{ij} tend to infinity within the physical region. Using (11) to (14), we obtain the following asymptotic expressions for the amplitude $F_{31}(\eta_{ij})$:

$$F_{31}(\eta_{ij}) \approx \begin{cases} \frac{1}{2} \pi C_{31} | \eta_{23} |^{-1/2} & \eta_{23} \gg | \eta_{12} |, | \eta_{13} | \\ h(\omega_{23}) C_{31} | \eta_{13} |^{-1/2} & -\eta_{13} \gg | \eta_{12} |, | \eta_{23} | \\ h(\omega_{23}^{-1}) C_{31} | \eta_{12} |^{-1/2} & -\eta_{12} \gg | \eta_{13} |, | \eta_{23} | \end{cases} \quad (17)$$

The function $h(\omega)$ is defined in the following way for $0 \leq \omega < \infty$:

$$h(\omega) = \begin{cases} \frac{1}{2} \left(\frac{\omega}{1-\omega} \right)^{1/2} \ln \frac{1 + \sqrt{1-\omega}}{1 - \sqrt{1-\omega}} & 0 < \omega < 1 \\ 1 & \omega = 1 \\ \left(\frac{\omega}{\omega-1} \right)^{1/2} \tan^{-1} \sqrt{\omega-1} & \omega > 1 \end{cases} \quad (18)$$

The behavior of the function $h(\omega)$ is shown in Fig. 6.

To obtain the asymptotic form of F_{31} as a function of the momentum transfer t_{xy} we must express the appropriate variable η_{ij} in terms of t_{xy} [formula (8)] and substitute in (17). It is seen from (17) that, as t_{xy} moves away from the singular point to values well inside the physical region, the

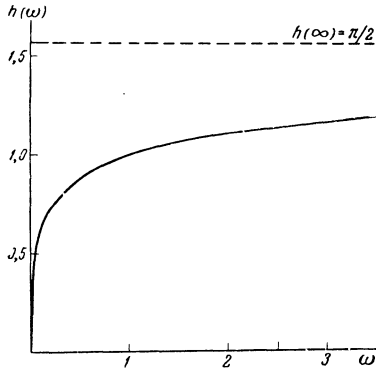


FIG. 6

amplitude of a triangular graph with constant vertices decreases more slowly (by a factor $\sim |t_{xy} - t_{xy}^0|^{-1/2}$, where t_{xy}^0 is the position of the singularity in t_{xy}) than the amplitude of the pole graph. As a rule, the singularities of triangular graphs lie about 2 to 3 times further removed from the physical region in t_{xy} than the poles.^[5] However, the slower decrease of $F_{31}(\eta_{ij})$ enhances the role of triangular graphs in the direct reaction mechanism.

We note that any conclusive discussion of the relative role of the pole and triangular graphs must take account of the momentum dependence of the vertex functions.

¹I. S. Shapiro, JETP **41**, 1616 (1961), Soviet Phys. JETP **14**, 1148 (1962).

²I. S. Shapiro, JETP **43**, 1727 (1962), Soviet Phys. JETP **16**, 1219 (1963).

³Blokhintsev, Dolinskii, and Popov, JETP **43**, 1914 (1962), Soviet Phys. JETP **16**, 1350 (1963).

⁴Blokhintsev, Dolinskii, and Popov, JETP **42**, 1636 (1962), Soviet Phys. JETP **15**, 1136 (1962).

⁵Blokhintsev, Dolinskii, and Popov, Nucl. Phys. (in press).

⁶P. V. Landshoff and S. B. Treiman, Nuovo cimento **19**, 1249 (1961).

⁷L. D. Landau, JETP **37**, 62 (1959), Soviet Phys. JETP **10**, 45 (1960).

⁸J. C. Polkinghorne and G. R. Sreaton, Nuovo cimento **15**, 289 and 925 (1960).

⁹L. M. Brown, Nuovo cimento **22**, 178 (1961).

¹⁰J. Tarski, J. Math. Phys. **1**, 149 (1960).

¹¹K. Yamamoto, Progr. Theor. Phys. **25**, 361 (1961).

¹²G. Källén and A. S. Wightman, Mat. Fys. Skrifter Dan. Vid. Selsk. **1**, No. 6 (1958).

¹³R. Oehme, Phys. Rev. **111**, 1430 (1958), Nuovo cimento **13**, 778 (1959).